Electronic Supplementary Information

Construction of covalent organic framework with unique double-ring pore for size-matching adsorption of uranium

Jie Zhang, [ab] Lihong Zhou,*[a] Zhimin Jia, [b] Xiaofeng Li, [b] Yue Qi, [b] Chuting Yang, [c] Xinghua Guo, [b] Shanyong Chen, [b] Honghan Long, [b] Lijian Ma*[b]

a. College of Environment and Ecology, Chengdu University of Technology, No.1, Dongsanlu, Erxianqiao, Chengdu 610059, P. R. China. E-mail: zhoulihong2012@cdut.edu.cn.

b. College of Chemistry, Sichuan University, Key Laboratory of Radiation Physics & Technology, Ministry of Education, No. 29 Wangjiang Road, Chengdu, 610064, P. R. China. E-mail: ma.lj@hotmail.com; Fax: +86 28 85412907; Tel: +86 28 85412329

c. Institute of Nuclear Physics and Chemistry, China Academy of Engineering Physics, Mianyang 621900, P. R. China.

* Corresponding Authors: ma.lj@hotmail.com (L. Ma); zhoulihong2012@cdut.edu.cn (L. Zhou).

Table of Content

Section S1. Synthesis of 1,3,5-triformylphloroglucinol (Tp)

Tp was synthesized following previously reported procedure.[1] Typically, phloroglucinol (6 g) and hexamethylenetetramine (15 g) in trifluoroacetic acid (75 mL) refluxed 2 h at 100 ℃, and then added the HCl (3 M,150 mL) refluxed 1-1.5 h. The characterizations of Tp were shown in Fig. S1-S3, and it were matched well with the literature.
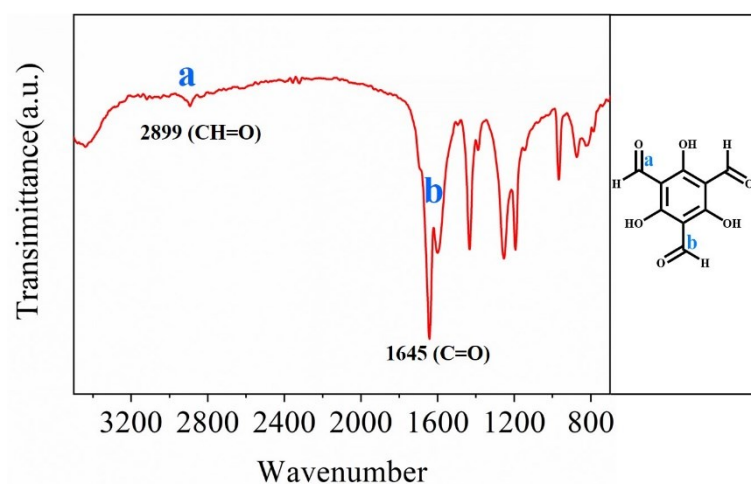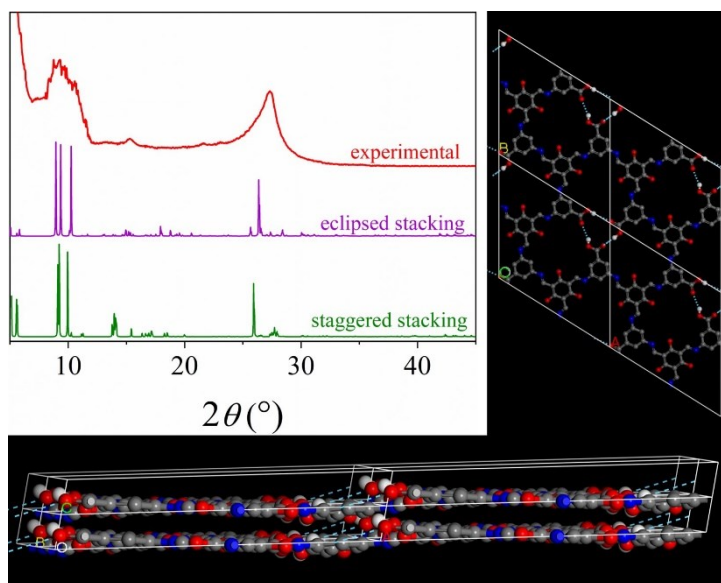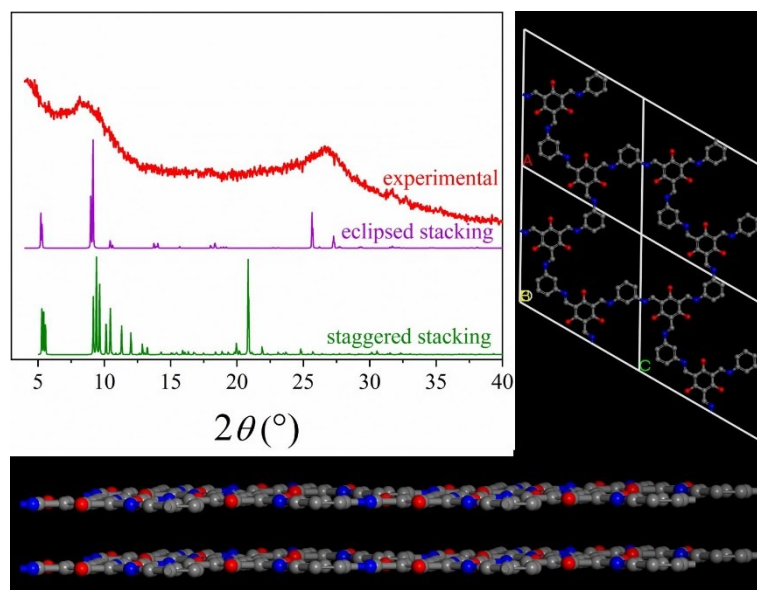

Fig. S1. FT-IR spectrum of Tp.
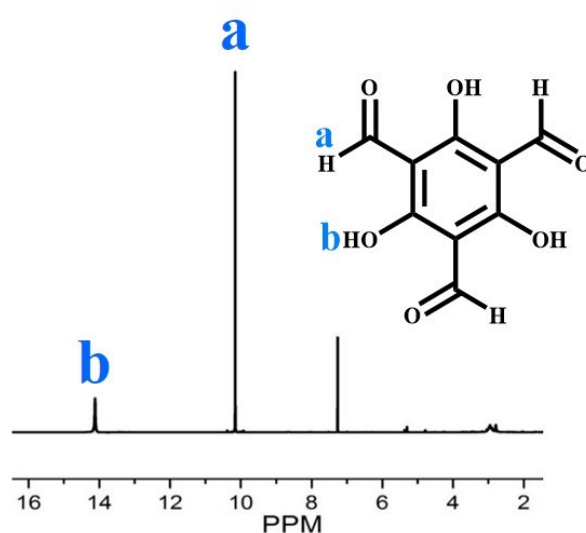
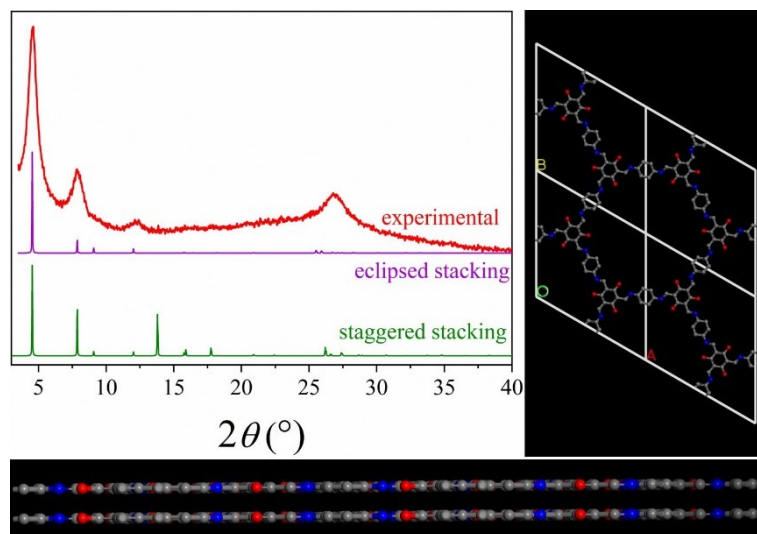**Fig. S2.** ^{1}H NMR spectrum (CDCl$_3$) of Tp.
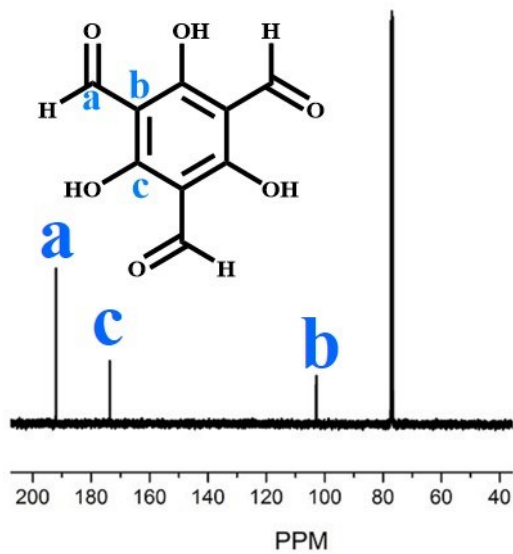
Fig. S3. ^{13}C NMR spectrum (CDCl$_3$) of Tp.

Fig. S4 Experimental and simulated PXRD patterns of Dp-COF, and space filling

models of Dp-COF with eclipsed stacking (C, gray; N, blue; O, red; H, white).
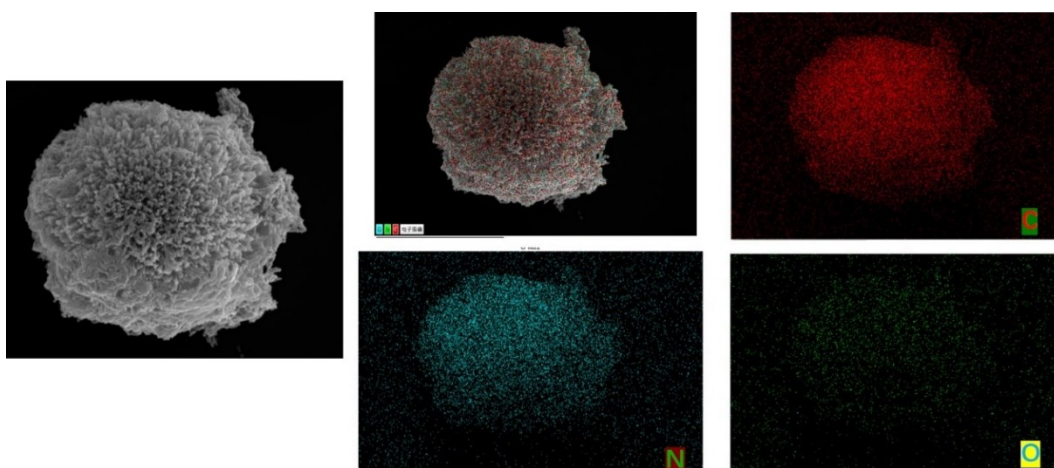
Fig. S5 Experimental and simulated PXRD patterns of TpMa, and space filling

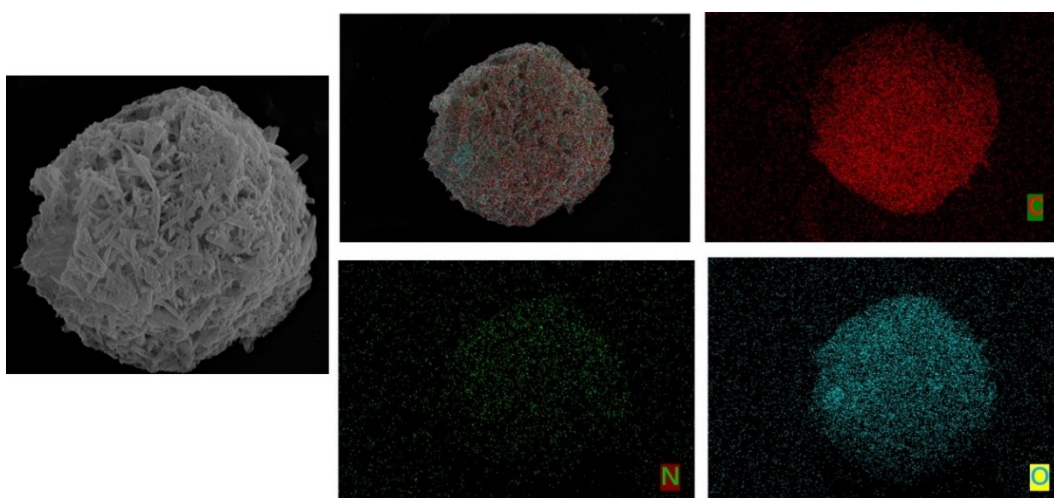models of TpMa with eclipsed stacking (C, gray; N, blue; O, red; H, white).

Fig. S6 Experimental and simulated PXRD patterns of TpPa-1, and space filling

models of TpPa-1 with eclipsed stacking (C, gray; N, blue; O, red; H, white).
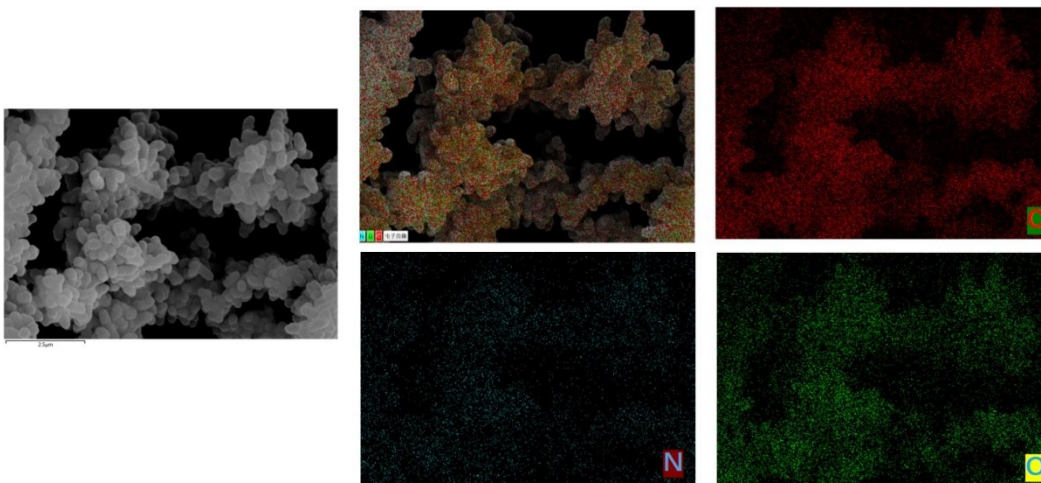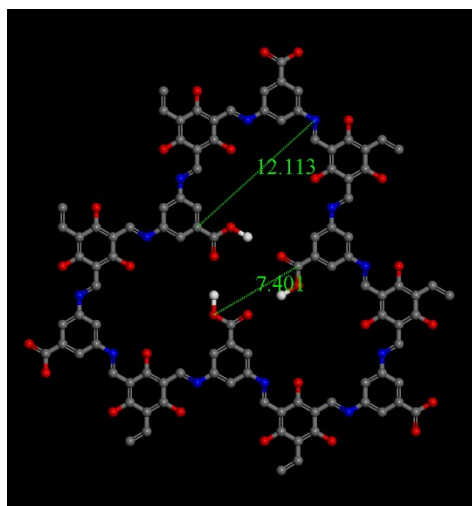
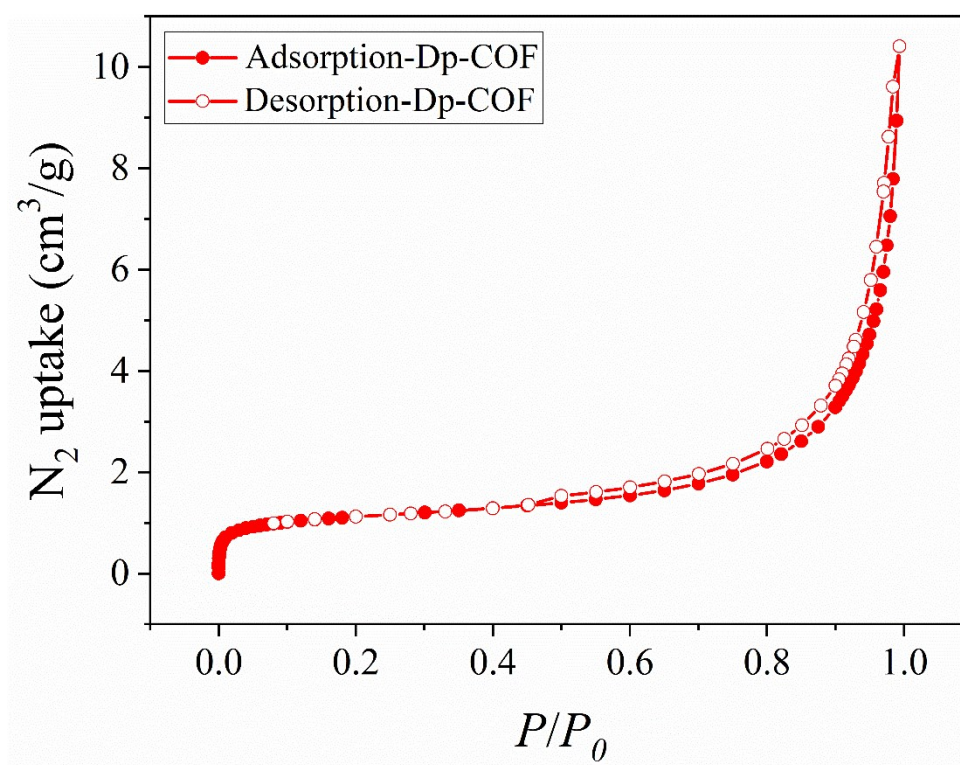**Fig. S7** SEM mapping images of Dp-COF.

Fig. S8 SEM mapping images of TpMa.
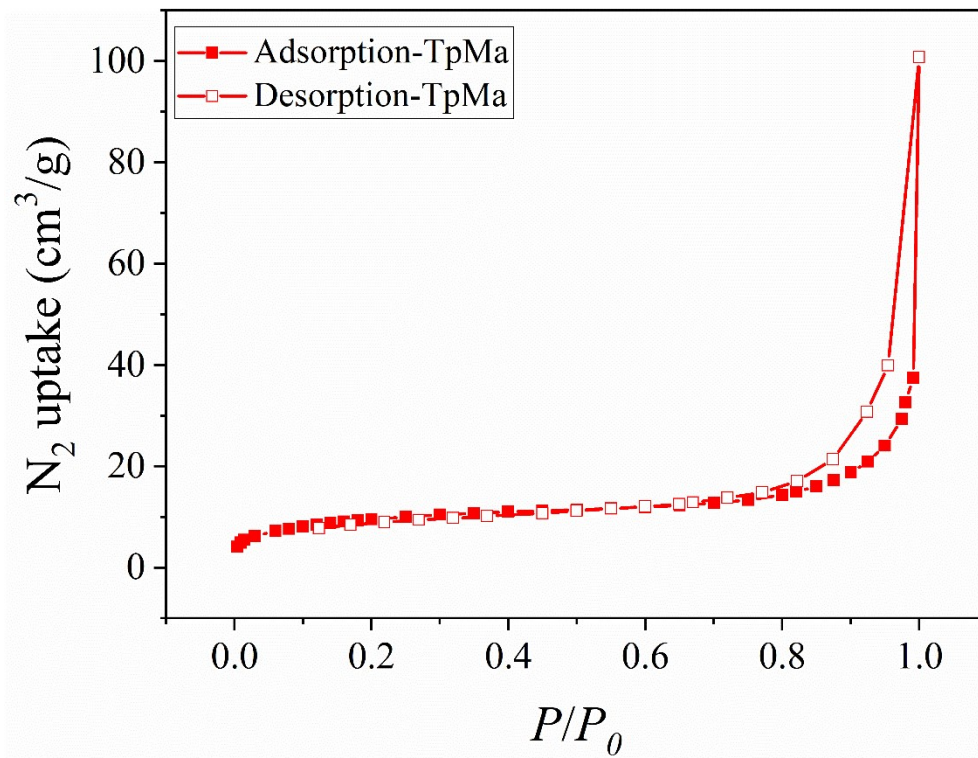

Fig. S9 SEM mapping images of TpPa-1.

Fig. S10 Simulated pore sizes of Dp-COF.

Fig. S11 N_2 adsorption–desorption isotherms of Dp-COF.

Fig. S12 N_2 adsorption–desorption isotherms of TpMa.
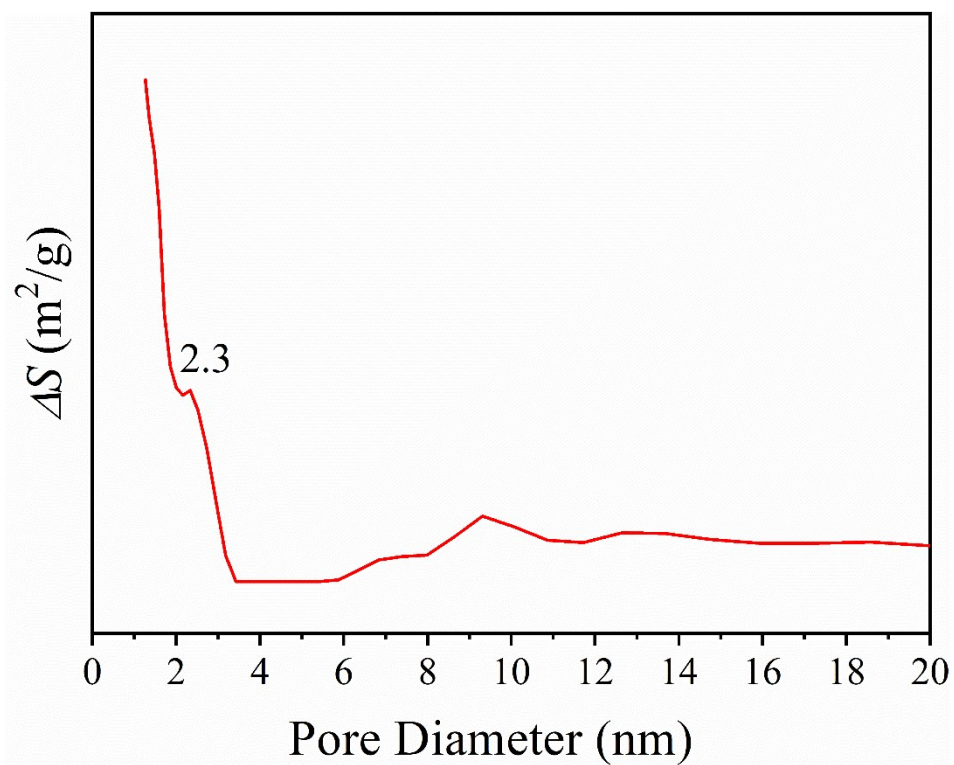
Fig. S13 Pore-size distribution of TpMa.
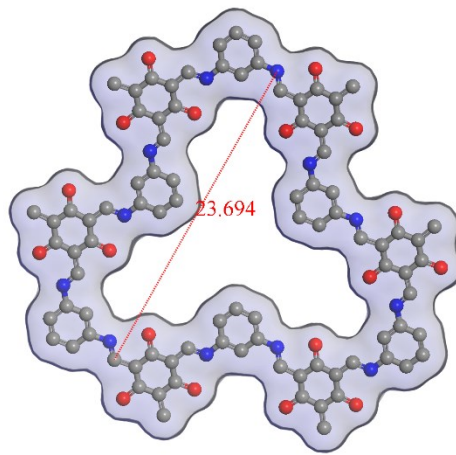
Fig. S14 Simulated pore sizes of TpMa.
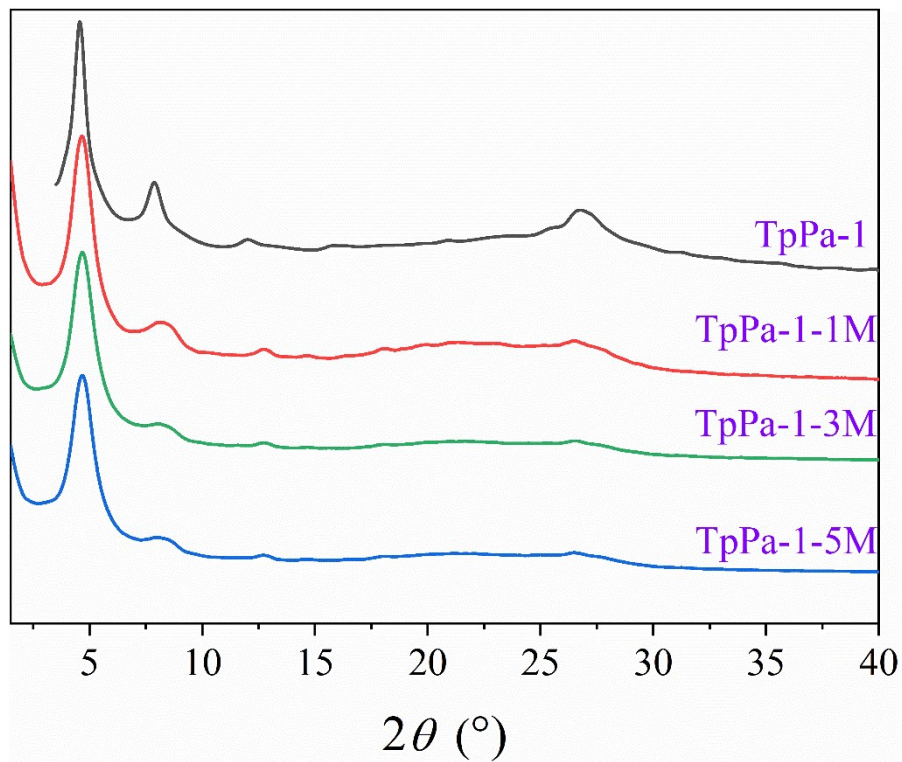
Fig. S15 XRD of TpPa-1 before and after soaking in HNO_3 solutions.
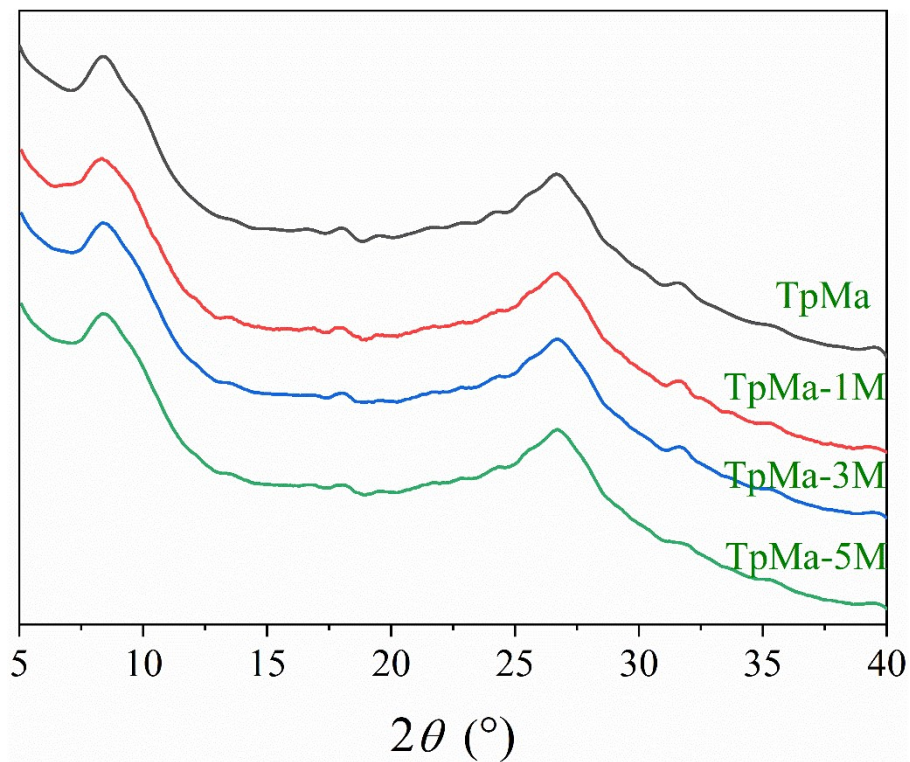
Fig. S16 XRD of TpMa before and after soaking in HNO_3 solutions.
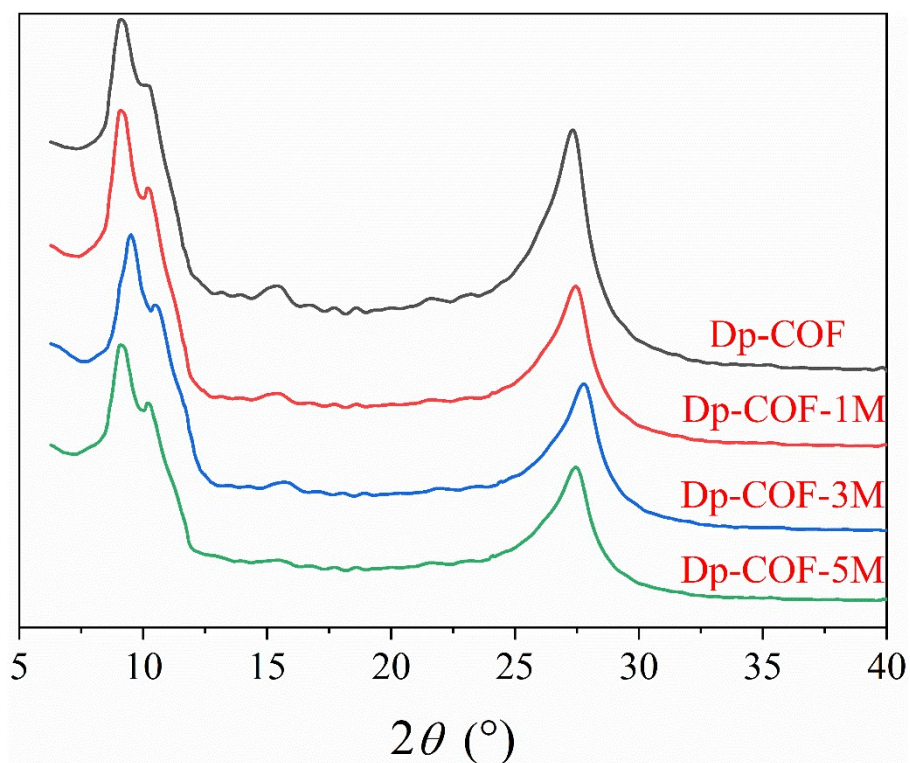
Fig. S17 XRD of Dp-COF before and after soaking in HNO_3 solutions.
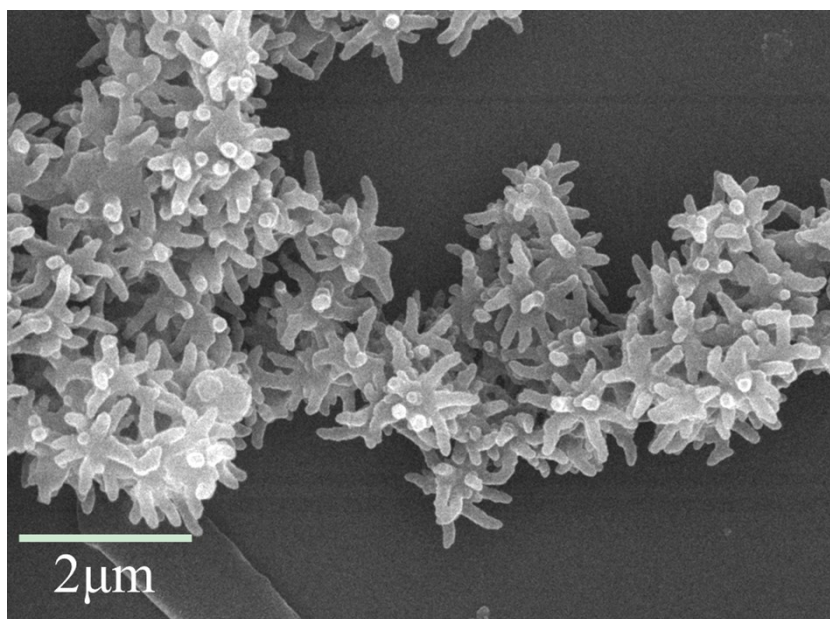
Fig. S18 SEM image of TpPa-1 after soaking in 5 M HNO_3 solution.
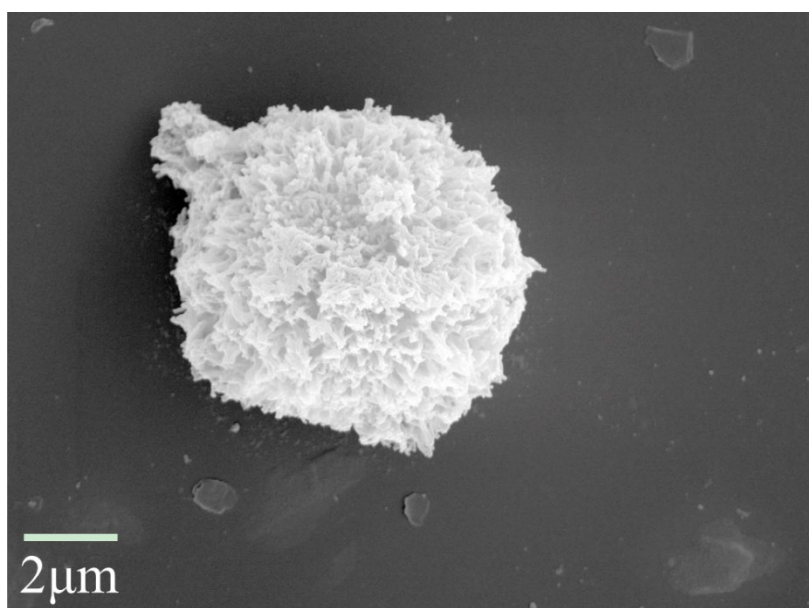
Fig. S19 SEM image of TpMa after soaking in 5 M HNO_3 solution.
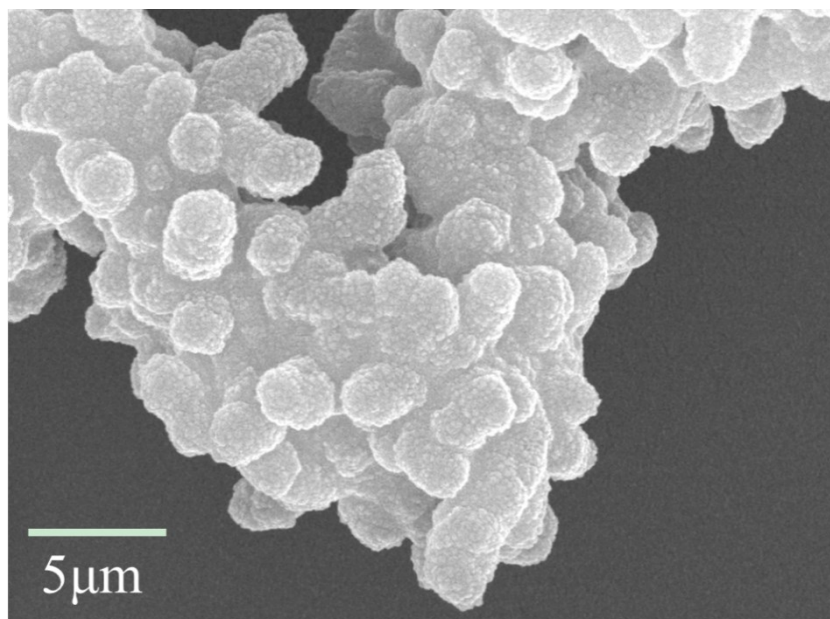
Fig. S20 SEM image of Dp-COF after soaking in 5 M HNO$_3$ solution.
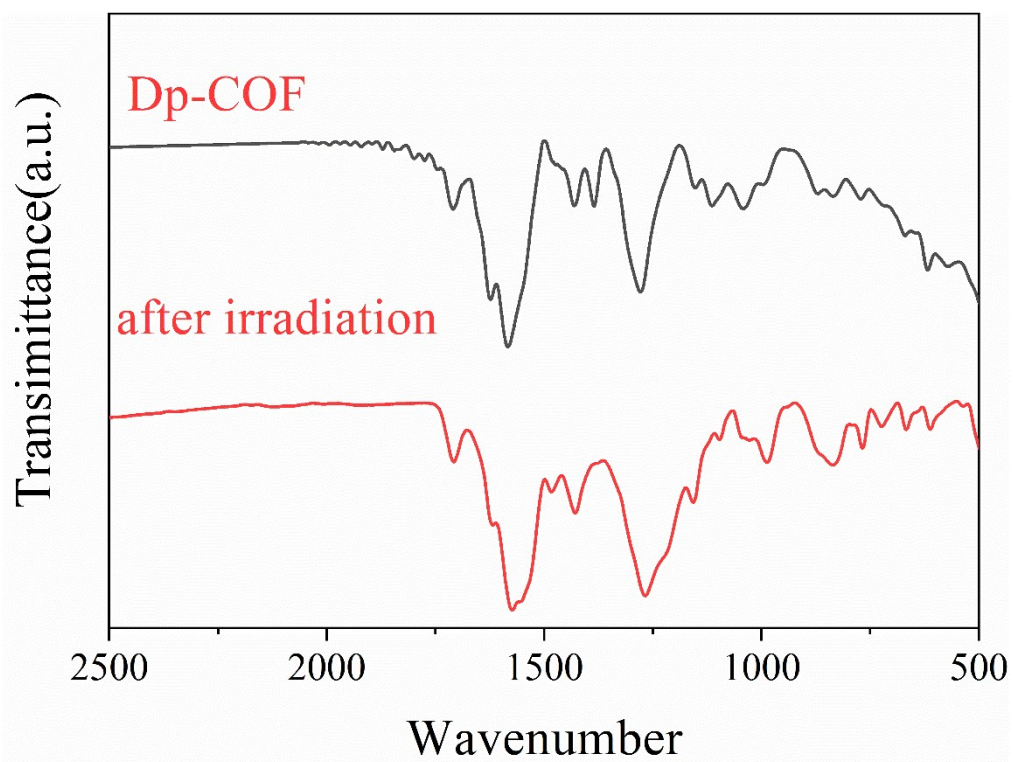
Fig. S21 FT-IR spectra of Dp-COF and Dp-COF after 10^5 Gy γ-ray irradiation.
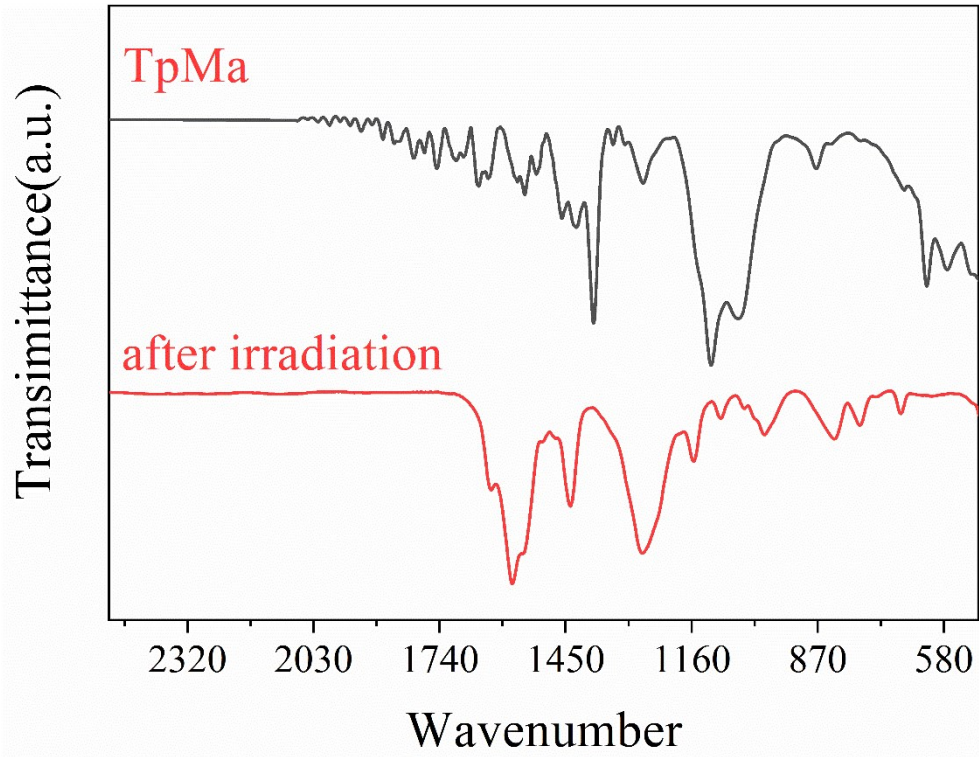
Fig. S22 FT-IR spectra of TpMa and TpMa after 10^5 Gy γ-ray irradiation.
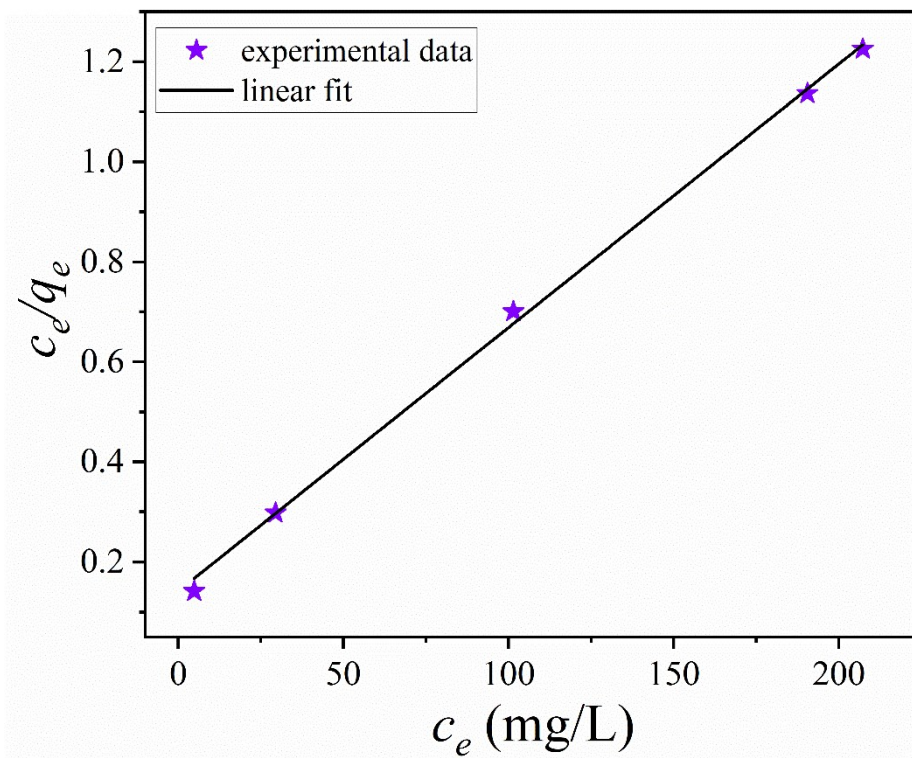
Fig. S23 Fitting curve for Langmuir model of TpPa-1.
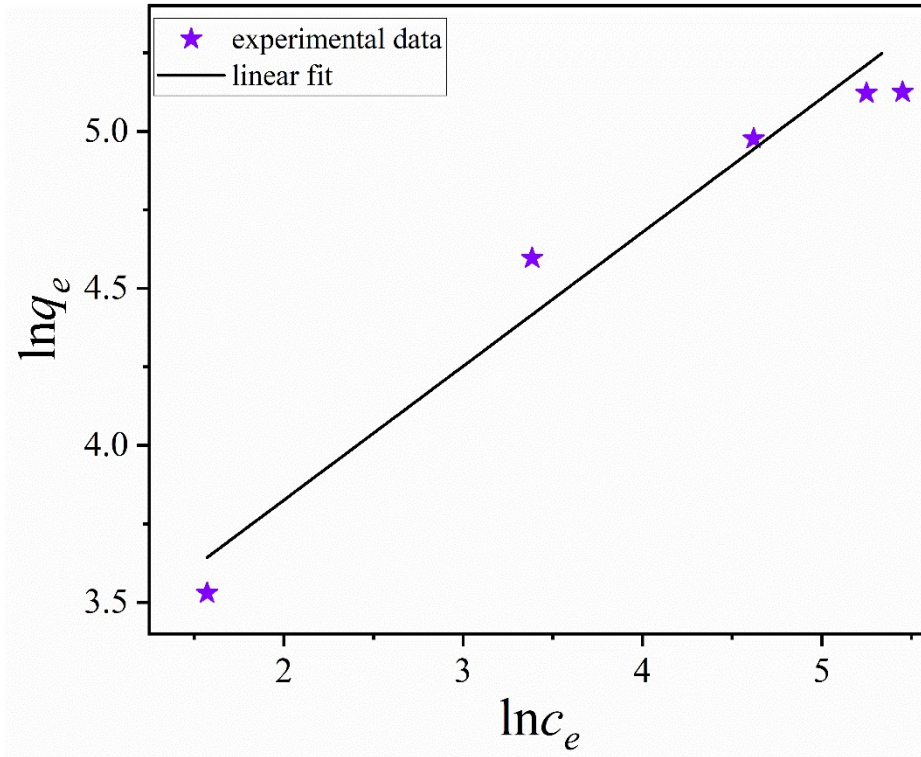
Fig. S24 Fitting curve for Freundlich model of TpPa-1.
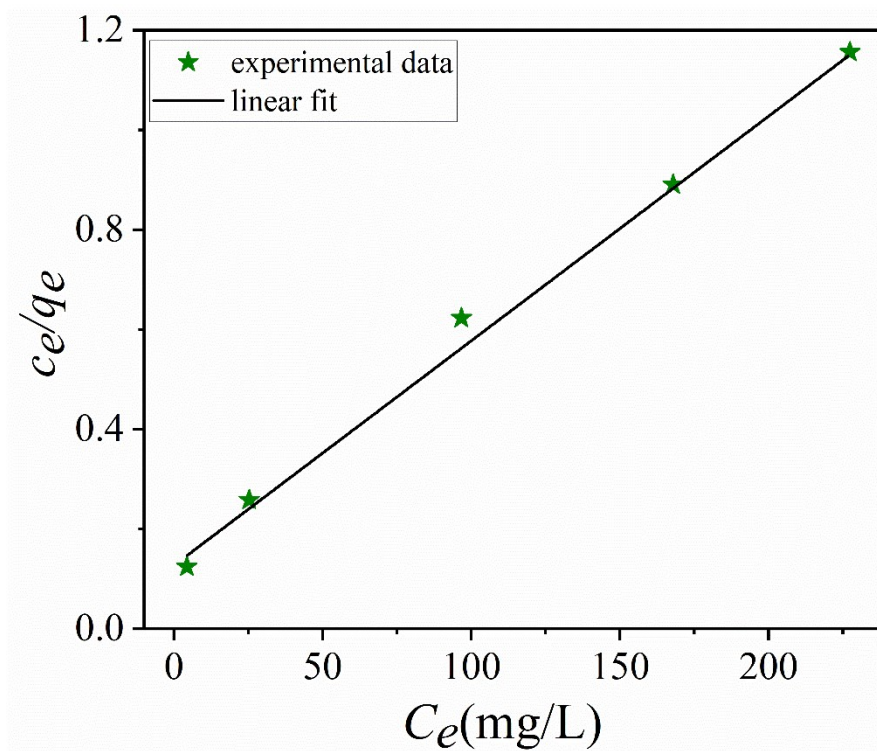
Fig. S25 Fitting curve for Langmuir model of TpMa.
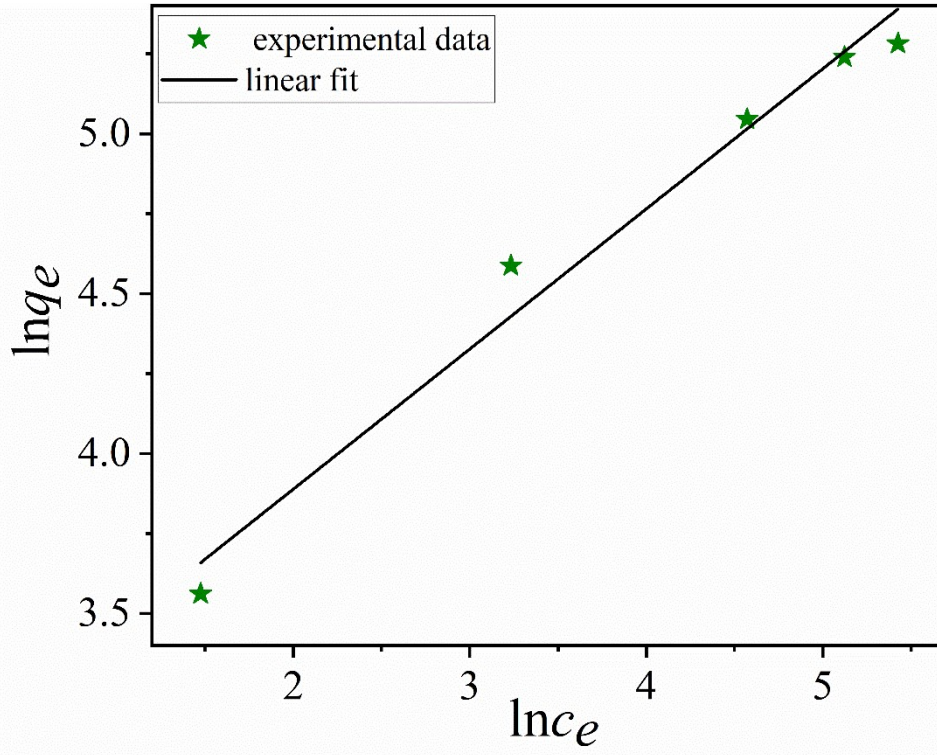
Fig. S26 Fitting curve for Freundlich model of TpMa.
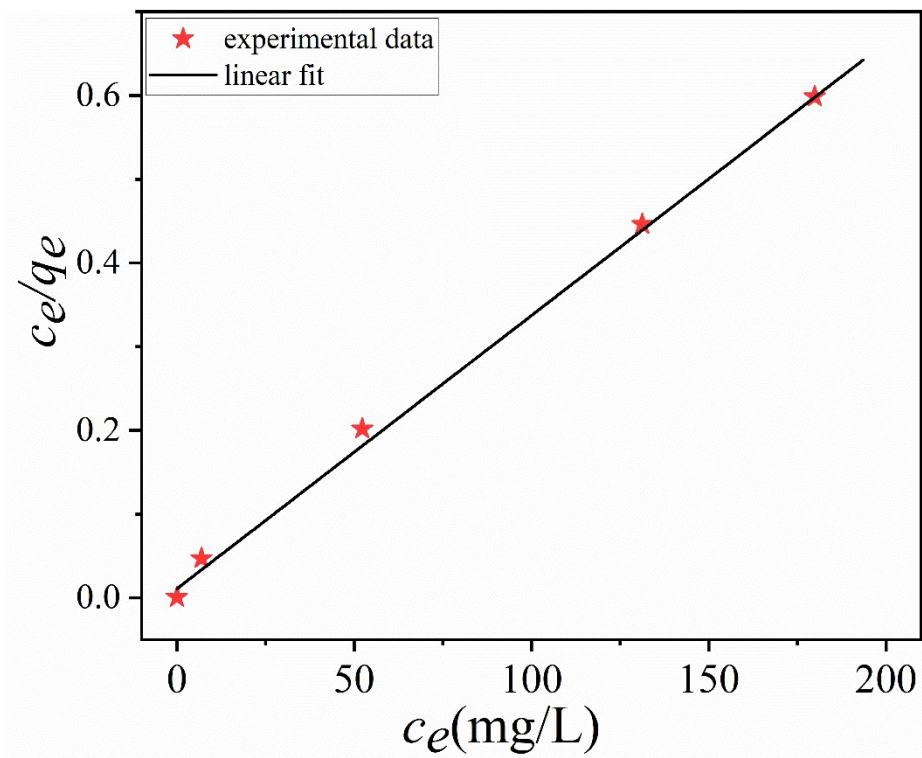
Fig. S27 Fitting curve for Langmuir model of Dp-COF.
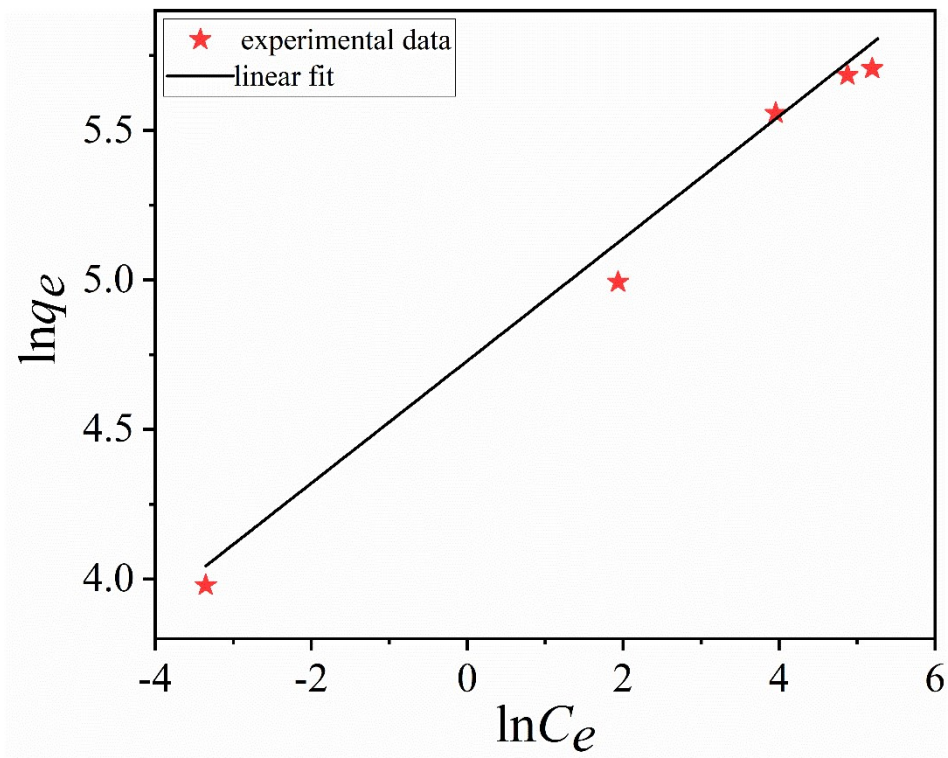
Fig. S28 Fitting curve for Freundlich model of Dp-COF.
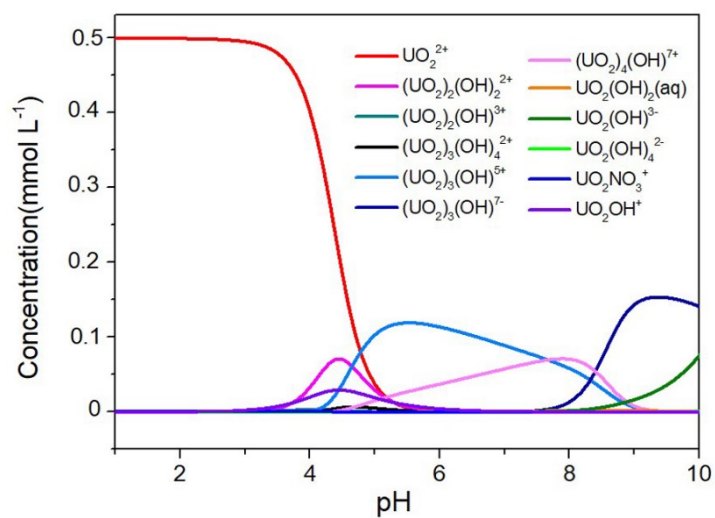
Fig. S29 The species distribution of uranium ($c_0 = 0.5$ mmol L^{-1}, $T = 25$ ℃) under

different pH conditions.
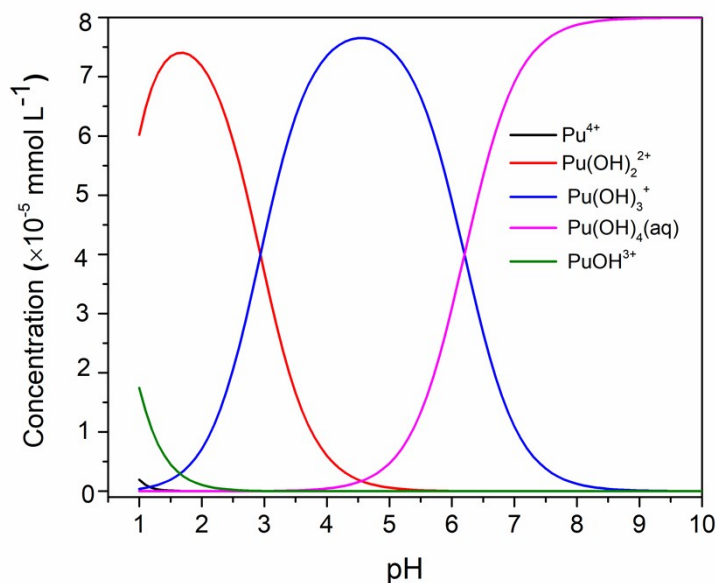
Fig. S30 The species distribution of plutonium ($c_0 = 8 \times 10^{-5}$ mmol L^{-1}, $T = 25$ ℃)

under different pH conditions.

Table S1. Result of elemental analysis.

Samples	C/wt %	H/wt %	N/wt %
TpPa-1	61.80	5.52	11.50
TpMa	59.89	4.16	11.29
Dp-COF	61.81	3.54	10.55

Table S2. Result of EDS

Samples	C/wt %	O/wt %	N/wt %
TpPa-1	51.65	38.63	9.72
TpMa	52.76	37.33	9.91
Dp-COF	48.17	38.21	13.61

Table S3. Compositions of the simulated nuclear industrial effluent.

Coexistent ion	Added as	Reagent purity
UO_2^{2+}	$UO_2(NO_3)_2 \cdot 6H_2O$	Standard reagent
La^{3+}	$La(NO_3)_3 \cdot 6H_2O$	99.9% metal basis
Ce^{3+}	$Ce(NO_3)_3 \cdot 6H_2O$	99.9% metal basis
Nd^{3+}	$Nd(NO_3)_3 \cdot 6H_2O$	AR
Sm^{3+}	$Sm(NO_3)_3 \cdot 6H_2O$	AR

Gd^{3+}	Gd(NO$_3$)$_3$·6H$_2$O	AR
Mn^{2+}	MnO	99.5%
Co^{2+}	Co(NO$_3$)$_2$·6H$_2$O	99.9% metal basis
Ni^{2+}	Ni(NO$_3$)$_2$·6H$_2$O	Spectrum pure
Zn^{2+}	Zn(NO$_3$)$_2$·6H$_2$O	99.9% metal basis
Ba^{2+}	Ba(NO$_3$)$_2$	99.9% metal basis

Table S4. Comparison of the adsorption capacities of U(VI) on Dp-COF and other reported adsorbents.

Sorbents	Experimental conditions	q_{max}(mg/g)	Ref
Dp-COF	T = 298 K, pH = 4.5	317	This work
COF-PDAN-AO	T = 298 K, pH = 4.0	256	2
COF-COOH	T = 298 K, pH = 4.5	211	3
COF-SO$_3$H	T = 298 K, pH = 5.0	360	4
o-GS-COF	T = 298 K, pH = 4.5	144	5
BDA-TN-AO	T = 298 K, pH = 5.0	526	6

Table S5. Isotherm parameters for the uranium adsorption onto TpPa-1.

isotherm model	parameter	value
	q_m (mg/g)	190
Langmuir	k_L (L/mg)	0.037
	R^2	0.997
	n	2.35
Freundlich	k_F (mg$^{1-(1/n)}$ L$^{1/n}$ g^{-1})	19.6
	R^2	0.964

Table S6. Isotherm parameters for the uranium adsorption onto TpMa.

isotherm model	parameter	value
Langmuir	q_m (mg/g)	222
	k_L (L/mg)	0.035
	R^2	0.998
Freundlich	n	2.28
	k_F (mg$^{1-(1/n)}$ L$^{1/n}$ g^{-1})	20.3
	R^2	0.977

Table S7. Isotherm parameters for the uranium adsorption onto Dp-COF.

isotherm model	parameter	value
Langmuir	q_m (mg/g)	307
	k_L (L/mg)	0.301
	R^2	0.999
Freundlich	n	4.89
	k_F (mg$^{1-(1/n)}$ L$^{1/n}$ g^{-1})	113.1
	R^2	0.976

Table S8. Radius (r) of the cations involved in the experiments.

ion	Gd[7]	Sm[7]	Mn[9]	Ba[7]	Ni[8]	Co[8]	Zn[8]	Ce[7]	Nd[7]	La[7]
r(Å)	1.34	1.33	0.83	1.39	0.69	0.75	0.74	1.34	1.34	1.32

Table S9. The experimental and theoretical data of the specific surface area and the total potential solvent area volume of Dp-COF and TpMa.

Samples	specific surface area		The total potential solvent area volume	
	theoretical value (m^2•g)	experimental value (m^2•g)	theoretical value(Å^3)	experimental value(Å^3)
TpMa	400.94	35.26	848.09	777.35

Dp-COF	94.97	90.18	599.31	856.38

References

1. J. H. Chong, M. Sauer, B. O. Patrick and M. J. MacLachlan, *Org. Lett.*, 2003, **5**, 3823-3826.
2. F. F. Li, W. R. Cui, W. Jiang, C. R. Zhang, R. P. Liang and J. D. Qiu, *J. Hazard. Mater.*, 2020, **392**, 122333.
3. J. Li, X. Yang, C. Bai, Y. Tian, B. Li, S. Zhang, X. Yang, S. Ding, C. Xia, X. Tan, L. Ma and S. Li, *J. Colloid Interface Sci.*, 2015, **437**, 211-218.
4. X. H. Xiong, Z. W. Yu, L. L. Gong, Y. Tao, Z. Gao, L. Wang, W. H. Yin, L. X. Yang and F. Luo, *Adv. Sci.*, 2019, **6**, 1900547.
5. R. Wen, Y. Li, M. Zhang, X. Guo, X. Li, X. Li, J. Han, S. Hu, W. Tan, L. Ma and S. Li, *J. Hazard. Mater.*, 2018, **358**, 273-285.
6. W. R. Cui, F. F. Li, R. H. Xu, C. R. Zhang, X. R. Chen, R. H. Yan, R. P. Liang and J. D. Qiu, *Angew. Chem. Int. Ed.*, 2020, **132**, 17837 – 17843.
7. F. David, V. Vokhmin and G. Ionova, *J. Mol. Liq.*, 2001, **90**, 45-62.
8. 1. R. D. Hancock and A. E. J. C. R. Martell, 1989, **89**, 1875-1914.
9. J. Luo, J. K. Liang, Q. L. Liu, F. S. Liu, Y. Zhang, B. J. Sun and G. H. Rao, *J. Appl. Phys.*, 2005, **97,** 068106.